Measurement of Erythrocyte Membrane Elasticity by Flicker Eigenmode Decomposition

H. Strey,* M. Peterson,‡ and E. Sackmann*
*Technische Universität München, Physik Department, Biophysik E22, 85748 Garching, Germany; and ‡Mount Holyoke College, South Hadley, Massachusetts 01075 USA

ABSTRACT We have studied the flickering of erythrocytes at wavelengths comparable to the cell dimension. To do this we have analyzed the edge fluctuations of the cell to a resolution of 5 nm by combining phase contrast microscopy with fast image processing. By measuring the edge excitations simultaneously at four orthogonal positions around the cell, the eigenmodes of equal azimuthal mode numbers $m = 0,1,2$ could be separated. From a continuous time sequence of 100 s of video frames taken at 40 ms time intervals, we determined the time-auto correlation function for the modes $m = 0,1,2$ and calculated their mean square amplitudes $\langle \delta n^2_m \rangle$ as well as their decay times τ_m. To explain the results we also present the theoretically calculated energy eigenmodes of an erythrocyte, accounting for the constraint that the cell is in contact with the substrate along an annular ring, which agreed well with the experimental findings. We found that the softest mode is a "hindered translational" mode with $m = 1$ of the adhered cell, which is almost insensitive to the shear elastic modulus. Comparison of the calculated and measured amplitudes yielded an average value for the bending stiffness of $k_c = 4 \times 10^{-19}$ J, which is much larger than the value obtained by flicker analysis at short wavelengths ($k_c = 2.3 \times 10^{-20}$ J). It would, however, agree well with the value expected from the red cell membrane area compressibility modulus of $K = 4.5 \times 10^{-1}$N/m, which corresponds to a lipid bilayer containing ~50 mol % of cholesterol. In contradiction to our theoretical expectations we found that the flicker eigenmodes seemed not to be influenced by the membrane shear elasticity, which will be discussed in terms of an unusual coupling between the lipid bilayer and the cytoskeleton.

INTRODUCTION

The puzzling question about the elastic properties of red blood cell (RBC) membranes has been around since 1975 when Brochard and Lennon (1975) suggested that the flicker phenomenon can be explained in terms of thermal undulations of the cell membrane. Their estimate of the bending modulus $k_c = 5 \times 10^{-20}$ J was based on the assumption that the red cell can be modeled by two fluctuating membranes that were parallel to each other. In this paper we show that to determine a more accurate and reliable value for the bending modulus one has to take into account the discoid biconcave equilibrium shape of RBCs. Because Brochard and Lennon (1975) considered flat membranes they neglected shear elasticity, which in this case enters the elastic energy in fourth order in normal displacement. But a red cell is not flat. In fact, there is no point on the cell with no curvature, and it can be shown that for a curved membrane the energies of shear deformations are second order in normal displacement and therefore should reduce the flicker amplitude (Peterson, 1985). If shear elasticity μ would be as high as reported from shear flow experiments $\mu = 1 \times 10^{-5}$N/m, (Hochmuth et al., 1973) or micropipet aspiration experiments $\mu = 6.6 \times 10^{-6}$N/m, by Waugh and Evans (1979) flicker should be much smaller. Since we see flicker there must be a low-shear regime for small shear deformations associated with thermal undulations.

In this paper we present a microscopic method to measure lateral edge fluctuations of an erythrocyte with a lateral resolution of 5 nm. This method determines the position of the refraction fringe ("halo"), which shows up at the edge of the cell, by using fast digital video image processing.

The mean square edge fluctuations of a total of ~900 nm^2 ± 25 nm^2 were measured very accurately at four points around a single cell to allow a mode decomposition according to the azimuthal mode number m. From the analysis of a 100-s real time video, which was processed at a rate of 25 images per second, we determined the mean square amplitudes of the first three azimuthal eigenmodes ($m = 0,1,2$) and their corresponding time autocorrelation functions.

The measured amplitudes were compared with theoretical calculations of the first few elastic eigenmodes of erythrocytes. The eigenmodes were constructed around a discoid biconcave equilibrium shape obeying both the constant area and constant volume constraint. We also had to take into account that during the experiments the cell was glued to a coverslip with an annular contact zone.

The largest eigenmode turned out to be a "hindered" translational mode with $m = 1$, which originated from the fact that the cell was glued to the coverslip. This mode was almost insensitive to shear elasticity and was therefore used to determine the membranes bending modulus k_c.

A typical value for the bending modulus of an individual cell was $k_c = 4 \times 10^{-19}$ J. This value is four times higher

Received for publication 11 October 1994 and in final form 24 April 1995.
Address reprint requests to H. Strey at his present address, National Institutes of Health, DIROD/National Institutes of Diabetes and Digestive and Kidney Diseases; and Laboratory of Structural Biology/Division of Computer Research and Technology, Bldg. 12A/2041, 12 South Dr MSC 5626, Bethesda MD 20892-5626. Tel.: 301-496-6562; Fax: 301-496-2172; E-mail: strey@helix.nih.gov.

0006-3495/95/08/478/11 $2.00

than the bending modulus found for artificial dimyristoyl phosphatidylcholine (DMPC) lipid vesicles (Duwe et al., 1990) and comparable to the bending modulus of a DMPC membrane containing 50% cholesterol (see discussion). A reasonable result, since the erythrocyte membrane consists of 50 mol % phospholipids and 50 mol % cholesterol (Wissenschaftliche Tabellen Geigy, Blut, Basel, Switzerland).

From the second largest mode with $m = 2$ (elliptical deformation) we determine the shear elasticity, since the amplitude of this mode should be sensitive to the membrane shear modulus. The measured shear elasticity μ was typically 100 times smaller than the static value measured by micropipet aspiration (Waugh and Evans, 1979). The fact that the $m = 2$ mode is not suppressed leads us to believe that the shear rigidity μ measured by micromechanical methods does not contribute to thermal shape fluctuations. It seems that for small shear deformations as in our case the shear resistance of the cytoskeleton vanishes.

MATERIALS AND METHODS

Microscopy

For our measurements we used a Zeiss Axiovert 10 microscope (Carl Zeiss, Oberkochen, Germany), for reflection interference contrast (RICM) as well as phase contrast and bright field microscopy. By changing the kind of illumination we were able to look at the same cells using RICM and phase contrast or bright field microscopy.

To view the adhesive contact area of the cells we used RICM (Rädler and Sackmann, 1993). Only cells showing a radial symmetric contact area between the cell and the coverslip were analyzed so that the theory (see Results and Appendix) could be applied (see Fig. 1).

Image processing system

The microscope pictures were taken by a charge coupled device camera (C2400, Hamamatsu, Hamamatsu City, Japan) at a rate of 50 half-images per second and recorded by an SVHS video recorder (Panasonic, Princeton, NJ). These images are digitized with 256 gray levels per pixel and processed by a fast image-processing system (Datacube, Boston, MA) depicted in Fig. 3.

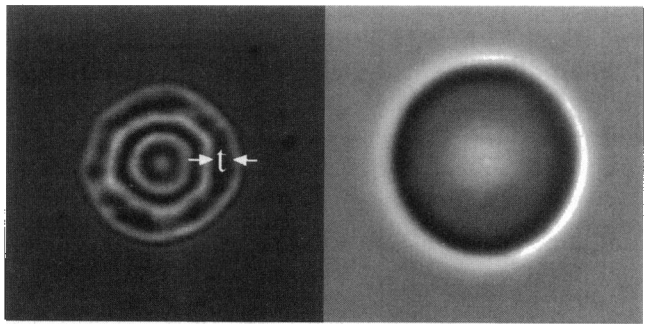

FIGURE 1 Reflection interference contrast micrograph (*left*) and phase contrast micrograph (*right*) of an erythrocyte in 290 mOsm buffer. In both cases the objective was focused on the bottom coverslip, which was coated with polylysine. Note the dark annular ring in the RICM image indicating where the cell is adhered to the surface. The arrows show the thickness t of the annular ring.

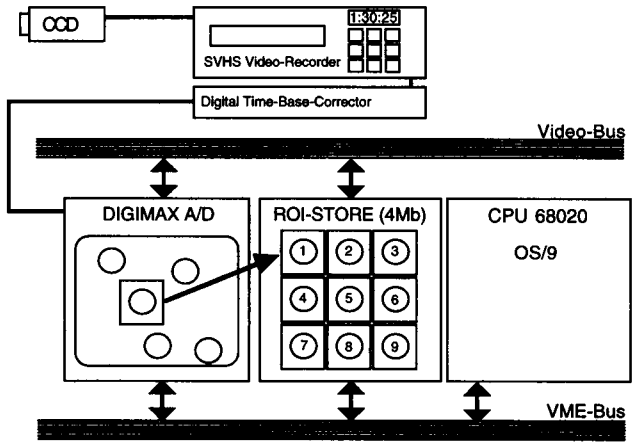

FIGURE 2 Schematic picture of the fast digital image processing computer (Datacube) used. The parallel structure of this computer allows to process user-defined regions of interest (ROI) in real time at full video rate.

For all our measurements we mapped 2 × 3 pixels to represent one point on the cell to reduce noise and to obtain quadratic pixel size (Fig. 2).

Method for estimating the lateral position of the cell edge

Phase contrast images of small objects exhibit strong diffraction fringes (halos), which result from the abrupt jump in index of refraction from the outer medium to the hemoglobin solution inside the cell. These halos are pronounced by the fact that some of the diffracted light is also retarded by the phase plate. The first fringe, therefore, reflects the position of the edge of the cell with a certain radial displacement.

To determine the position of the halo we used two methods. Fig. 3 shows the radial intensity profile at the edge of an RBC. The position of the edge can then be measured by interpolating the lateral position at which a certain predefined threshold intensity is reached. This method is very robust but sensitive to fluctuations of illumination.

Another possibility is to take the derivative of the intensity profile in the radial direction and to estimate its root (Fig. 4).

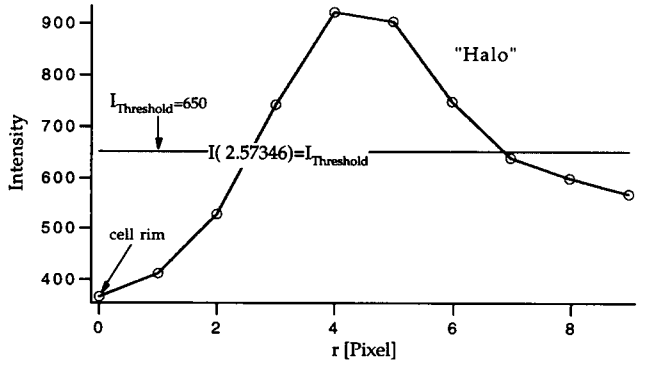

FIGURE 3 Radial intensity distribution profile of phase contrast micrograph at the rim of the cell showing a strong diffraction fringe (halo) beyond the cell edge. $r = 0$ approximately defines the rim of the cell. The radial position of the edge can be determined very accurately by estimating the radial position where the intensity reaches a certain threshold value between the minimum and the maximum intensity of the halo.

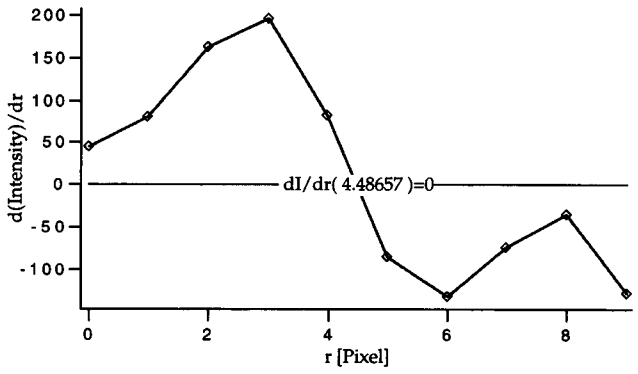

FIGURE 4 Derivation of the intensity profile (Fig. 3) in radial direction. $r = 0$ approximately defines the rim of the cell. The radial position of the cell edge can be alternatively determined by estimating the position where $dI/dr = 0$ defining the position where the halo is maximal in intensity.

Because we observe single erythrocytes, the resolution measuring the position of the edge of the cell is no longer dependent on the optical resolution of the light microscope but rather is determined by noise. This kind of "ultramicroscopy" or "superresolution" (see, e.g., Inoué, 1989) is well established for tracking particles smaller than the wavelength of light and for observing filaments with a few-nanometer thickness, such as microtubulin or actin. By measuring the camera noise and performing a straightforward error calculation we estimated a lateral resolution of 5 nm. This means that for a typical flicker amplitude of $(30\ \text{nm})^2$ the relative error of our measurement would be $(5\ \text{nm})^2/(30\ \text{nm})^2 = 3\%$.

Azimuthal mode decomposition

Mode decompositions were performed by measuring the lateral edge fluctuations at four equally spaced points around the cell as shown in Fig. 5. The positions of the four cell edges were determined simultaneously over 2500 full frames or 100 s as described in the section titled Method for Estimating the Lateral Position of the Cell Edge.

In some cases the data showed long time drifts of the coverslip relative to the objective. These drifts showed up as a constant slope superimposed on the data. In these cases opposite points (1,3 and 0,2 in Fig. 5) showed the same slope, which clearly indicated that the coverslip was drifting. None of the measured cells ever moved relative to the coverslip. To eliminate the drift, we subtracted a line fit from the data at each location.

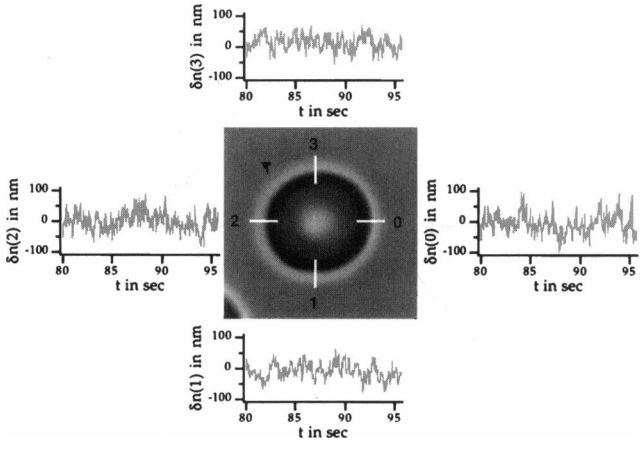

FIGURE 5 Azimuthal Decomposition: the lateral edge fluctuations δn were measured simultaneously at four points, $\delta n(0)$, $\delta n(1)$, $\delta n(2)$, and $\delta n(3)$, around the cell. For each time the azimuthal modes $\delta n_{m=0}$, $\delta n_{m=1}$, and $\delta n_{m=2}$ were calculated by a discrete Fourier transform of the four points. From a continuous time sequence the time-autocorrelation function of modes with $m = 0$, $m = 1$, and $m = 2$ could be calculated.

Because of small deviations from the cylindrical symmetry of the cell or its contact area the mean square amplitudes measured at four points around the cell were slightly different. Therefore only cells that showed a <10% difference in the four mean square amplitudes were considered. To account for the difference we normalized each of the four time series to have the same mean square fluctuations by multiplying each by an appropriate constant. This was necessary to obtain time-autocorrelation functions that properly drop off in time.

Next we Fourier-transformed the four fluctuation amplitudes $\delta n(0)$, $\delta n(1)$, $\delta n(2)$, and $\delta n(3)$ with respect to the azimuthal mode number m for each time.

$$\delta n_m = \frac{1}{4}\sum_{n=0}^{3} \delta n(n) e^{i2\pi nm/4} \qquad (1)$$

The first three azimuthal modes are shown schematically in Fig. 6. The mode with $m = 0$ represents a radius fluctuation, $m = \pm 1$ a translation of the whole cell, and $m = \pm 2$ an elliptical deformation.

The complex Fourier amplitudes δn_m (with $m = -2, -1, 0, 1, 2$) were then used to calculate the time autocorrelation function $K_m(t')$ according to Eq.2:

$$K_m(t') = \frac{1}{N}\sum_{n=0}^{N-1} \delta n_m(t = n\Delta t)\delta\overline{n_m}(t = n\Delta t + t') \qquad (2)$$

where Δt is the video sampling rate of 40 ms. The time autocorrelation functions taken at $t' = 0$ represent the mean square amplitudes $K_m(t' = 0) = \langle \delta n^2{}_m \rangle$ for each mode m.

According to the sampling theorem (Press et al. 1988) the mode decomposition is not exact because of aliasing. This means that all modes with anazimuthal mode number greater than $m = 2$ contribute to the measured amplitudes $\delta n_{m=0}$, $\delta n_{m=1}$, $\delta n_{m=2}$. Thus, the measured means square amplitude $\langle \delta n^2{}_{m=2} \rangle$ actually is the sum of the mean square amplitudes of $m = \pm 2, \pm 6, \pm 10$, ..., whereas $\langle \delta n^2{}_{m=1} \rangle$ is the sum of $m = \pm 1, \pm 3, \pm 5$, ..., and $\langle \delta n^2{}_{m=0} \rangle$ is the sum of $m = 0, \pm 4, \pm 8$, ... This aliasing effect on the interpretation of the measured amplitudes will be discussed in detail in the Results section.

RESULTS

Experimental mode decomposition

Fig. 7 shows the time autocorrelation functions $K_{m=0}(t)$, $K_{m=1}(t)$, and $K_{m=2}(t)$ of the first three azimuthal modes with $m = 0,1,2$ of an RBC with an average membrane elasticity. Because we Fourier-transformed a real-valued sample we used $K_{m=1}(t) = K_{m=-1}(t) + K_{m=1}(t)$ and $K_{m=2}(t) = K_{m=-2}(t) + K_{m=2}(t)$.

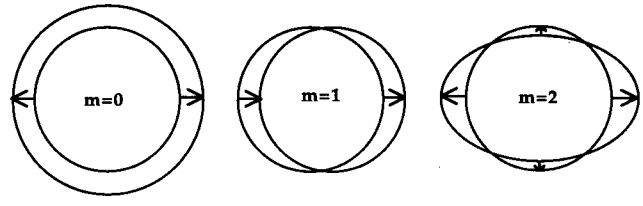

FIGURE 6 Schematic view of fluctuations of the cell rim with azimuthal symmetries $m = 0,1,2$.

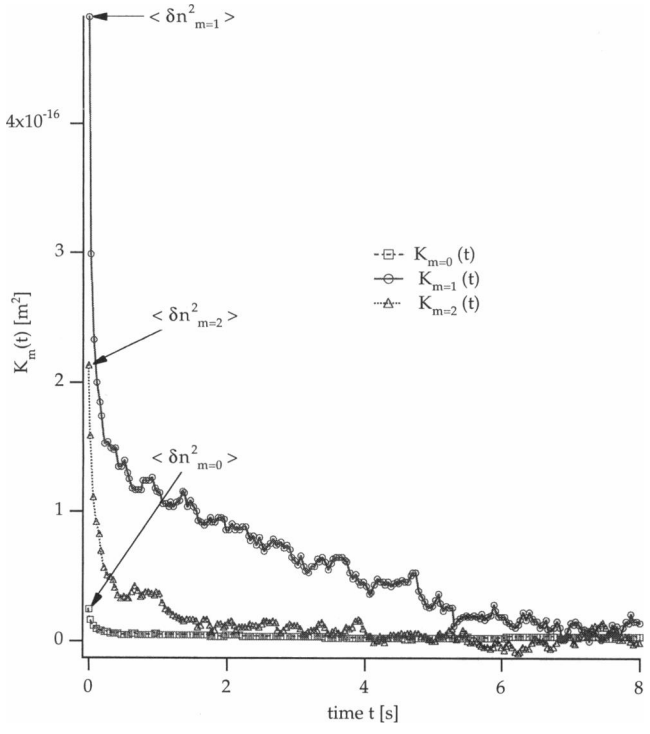

FIGURE 7 Time correlation functions $K_m(t)$ of Fourier component δn_m (with m = 0,1,2) of the edge fluctuation for an erythrocyte kept at 290 mOsm. The maximal amplitudes (t = 0) are indicated by arrows.

The mode decomposition clearly shows that the translational mode with $m = 1$ is the dominating one with a mean square amplitude of 600 nm^2. The elliptical mode with m = 2 is three times smaller than the translational mode, and the mode with $m = 0$ is 10 times smaller.

Assuming that all errors are independent of the azimuthal mode number m we can divide the total error of (5 nm)^2 by three to get the absolute error of each mode. The relative error of the translational amplitude with $m = 1$ is then 1.4%, for the elliptical mode with $m = 2$ it is 2% and for the mode with $m = 0$ it is ~30%.

All three autocorrelation functions decay exponentially in time, $K_m(t) = a\, e^{-t/\tau}$, as expected from the fluctuation-dissipation theorem (see, e.g., Reichl, 1980) applied to a harmonic oscillator in a viscous medium. The mode with m = 2 decays with τ = 44 ms and the $m = 0$ mode decays with τ = 37 ms.

It should be noted that the translational mode ($m = 1$) shows a two-exponential decay $K_m(t) = a_1\, e^{-t/\tau 1} + a_2\, e^{-t/\tau 2}$ with two distinguishable decay times of τ_1 = 2.7 s and τ_2 = 86 ms. The slow decay (high viscosity) can be completely removed by focusing on the top of the cell. This suggests that the damping of the undulations varies from the top to the bottom of the cell. While the upper membrane is coupled to an infinite half space of buffer, the lower membrane senses the thin buffer layer between the cell surface and the coverslip.

It should be noted that in cases where the time correlation function decays faster than the sampling rate (or the time the signal was integrated to get a single data point) the resulting amplitude is smaller than if one were to sample at a higher rate (Faucon et al., 1989). In our case the decay times were reasonably close to the sampling time of 40 ms, so that there was no need to correct for the integration time of the camera.

Theoretical mode spectrum of an erythrocyte adhered to a coverslip

In our previous theoretical analysis (Peterson et al., 1992) in which we described the eigenmode spectrum of a freely floating cell, we neglected all translational and rotational motions of the cell because they did not cost deformation energy. The experimental analysis of the flicker was based on the evaluation of the thickness fluctuation profile where all modes with $l + m$ even are summed, so that a distinction between different modes was not possible. Through comparison of the measured thickness fluctuation profile along the diameter of the cell with the theoretically predicted one we concluded that the influence of shear on RBC flicker is negligible. In this case the Goldstone mode with $l = 2, m$ = 2 would be the largest mode.

The results of our mode decomposition presented here showed that in contrast to our first analysis the mode with m = 1 (translation) dominates the flicker spectrum. This experimental fact led to the idea to calculate the eigenmodes of a cell adhered to the bottom of the measuring chamber.

Fig. 1 shows an RICM image together with a phase contrast micrograph image of the same RBC. Generally, the RICM shows the contour lines of the lower side of an object as interference rings (Newton rings). The dark broad band (area between the two arrows) in the RICM image represents the contact area where the cell adheres to the poly-lysine-coated coverslip.

As shown in Fig. 1 this contact area can to good approximation be described by an annular ring with thickness t where the cell thickness is maximal (see also Fig. 8). At this contact area the membrane is constrained not to move normal to the cell membrane. The cell adheres to a poly-lysine layer deposited on the coverslip via electrostatic interactions of the negatively charged sugar groups of gly-

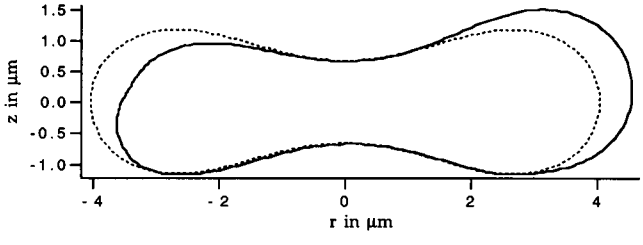

FIGURE 8 Shape change of RBC caused by "hindered translation" mode with m = 1. The dashed line represents the equilibrium shape. The amplitude of the mode shown in this figure is ~100 times the measured mean square displacement. This was done to illustrate the features of the "hindered translation".

coproteins with the positively charged lysine groups. Since the membrane remains in the fluid state tangential flow of the lipid component of the membrane is, however, still possible. It is obvious that the thickness t of the annular ring of contact will significantly influence the amplitude of the membrane fluctuations, because the contact area reduces the total area that is able to flicker freely. In the Appendix we show how to formulate the constraint theoretically and how to solve the eigenmode spectrum accounting for the above constraint.

The theoretical calculation of the eigenmode spectrum shows that through this new constraint, a translational mode with $m = 1$ survives as an eigenmode, which we call "hindered translation mode." This mode is shown in Fig. 8, where the dashed line represents the equilibrium shape of the RBC.

Fig. 9 shows the theoretically expected azimuthal mode distribution at the edge of the cell δN (δN denotes a theoretically predicted value, whereas δn is measured) as a function of the thickness t of the annular ring and the parameter $\epsilon = \mu R^2/k_c$, the dimensionless ratio of shear and bending elasticity. R is the equivalence radius with respect to the cell volume $V = 4\pi/3\ R^3$ ($R = 3.017\ \mu$m at 290 mOsm for an average cell). The mean square amplitudes of each azimuthal mode is expressed in units of $\langle \delta N^2_m \rangle k_c / k_B T R^2$ so that measuring the absolute value of the mean square amplitude $\langle \delta n_m^2 \rangle$ for any mode yields the bending elasticity k_c of the red cell membrane.

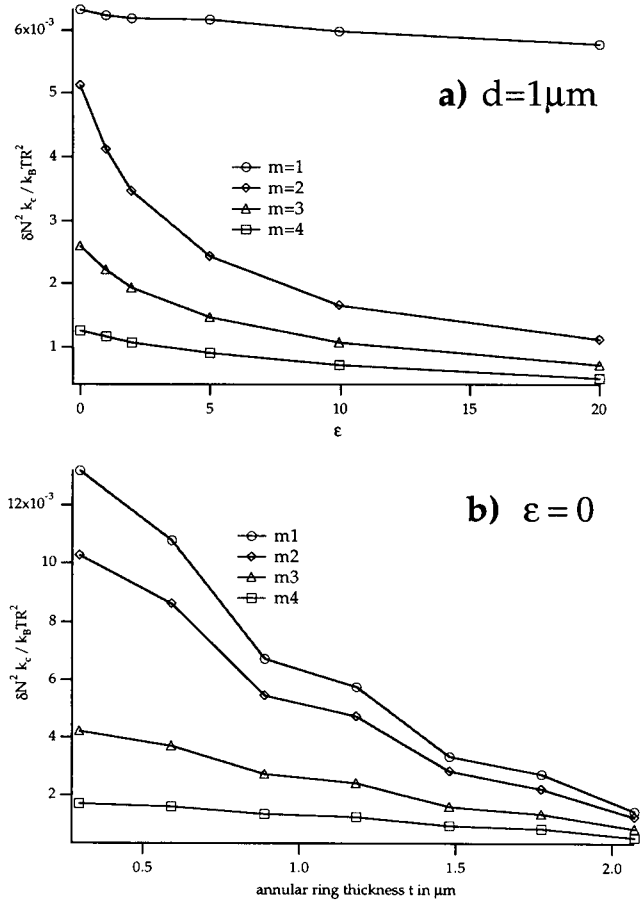

FIGURE 9 Theoretical edge fluctuations of a cell kept at 290 mOsm with respect to the azimuthal mode number m as a function of $\epsilon = \mu R^2/k_c$ and the thickness t of the annular ring of contact.

We did not show the modes with $m = 0$, because this mode is strongly suppressed by both volume and area constraint. Since the additional bilayer coupling hypothesis constraint (see Appendix) only shows up in modes with $m = 0$, all shown modes in Fig. 9 were independent of the used membrane model (for an explanation of the bilayer coupling hypothesis or spontaneous curvature model, see Peterson et al., 1992).

The translational mode with $m = 1$ is almost independent of the shear elasticity μ. The amplitudes of all other modes $m = 2,3, \ldots$ decay strongly with increasing μ. This behavior suggests a procedure to estimate both bending elasticity k_c and shear elasticity μ by measuring the absolute amplitudes of the modes with $m = 1$ and $m = 2$. The bending elasticity is obtained from the absolute amplitude of the $m = 1$ mode and $\epsilon = \mu R^2/k_c$ can then be estimated from the ratio of $m = 1$ and $m = 2$.

Measurement of bending modulus k_c and shear modulus μ of a red cell membrane for long wavelength excitations by mode decomposition

The comparison of our theoretical results with our mode decomposition measurements of erythrocytes was done as follows. We first measured the average thickness t of the annular contact ring of the RBC by determining the contact area from the RICM image (see Fig. 1). The contact zone where the RBC is adhered to the polylysine shows in the RICM image as a dark region and can therefore easily be measured. The thickness t can then be calculated from both the area and the radius of the ring.

To obtain the theoretical flicker amplitudes at the edge of the cell $\langle \delta N^2_m \rangle$ for this particular thickness we interpolated its value from a set of calculated amplitudes for thicknesses 0.5, 1, 1.5, and 2 μm.

We then determined ϵ from the ratio of $\langle \delta n^2_{m=1} \rangle$ to $\langle \delta n^2_{m=2} \rangle$. Because $\langle \delta n^2_{m=1} \rangle$ is the sum of contributions from approximately $m = 1$ and $m = 3$ we interpolated the theoretical ϵ dependence of the edge fluctuations (see Fig. 9) $\langle \delta N^2_{m=1} \rangle + \langle \delta N^2_{m=3} \rangle / \langle \delta N^2_{m=2} \rangle$ to give the measured ratio.

This ϵ was used to interpolate the value of the theoretical mean square flicker amplitude $(\langle \delta N^2_{m=1} \rangle + \langle \delta N^2_{m=3} \rangle) k_c / k_B T R^2$, from which we calculated the bending resistance k_c using $\langle \delta N^2_{m=1} \rangle + \langle \delta N^2_{m=3} \rangle = \langle \delta n^2_{m=1} \rangle$, the measured equivalence cell radius R and $k_B T = 4 \times 10^{-21}$ J. The shear modulus μ was then obtained from the value of $\epsilon = \mu R^2/k_c$.

For two cells the ratio of $\langle \delta n^2_{m=1} \rangle$ to $\langle \delta n^2_{m=2} \rangle$ could not be explained by the theoretical results for positive ϵ, and μ therefore was set to zero. Nevertheless the deviations from the theoretical predictions were so small that the bending modulus calculated for $\mu = 0$ was still reasonable.

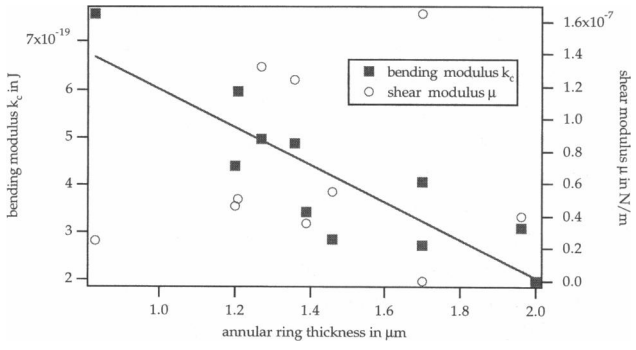

FIGURE 10 Measured bending modulus k_c and shear modulus μ of 11 erythrocytes plotted against their annular ring thickness t. Interestingly, the bending modulus seemed to be almost linearly dependent on the annular ring thickness, whereas the shear modulus μ was quite variable.

Fig. 10 shows results from 11 erythrocytes from two donors under physiological buffer conditions. We plotted both the bending modulus k_c and the shear modulus μ against the thickness t of the annular ring. From the plot it seemed that the bending modulus was strongly correlated to the thickness of the annular ring t. This is quite plausible because cells with a smaller k_c would be less able to maintain their normal equilibrium shape against adhesive forces from the substratum and therefore would show a larger contact area. The values for the bending modulus cover the range from 2×10^{-19} J to 7×10^{-19} J. This is not very surprising considering that erythrocytes show a wide range in composition of the lipid bilayer (Wissenschaftliche Tabellen Geigy, Blut) and in age. For us it was more surprising that no one before quantified larger differences in membrane elasticity of different red cells (Linderkamp and Meiselman, 1982). Just looking at the flicker motion through a microscope, especially with RICM, it was obvious to us that there must be a large variation in cell elasticities. Smaller and presumably older cells adhere with a smaller contact area and show smaller flicker amplitudes, whereas larger and younger cells adhere with a larger contact area and show stronger thermal fluctuations.

The shear moduli determined by our method did not seem to depend on the annular ring thickness t. The values of the shear modulus μ ranged from 0 to 1.6×10^{-7}N/m, and were very scattered. Typically the shear modulus was about 100 times smaller than inferred from micromechanical experiments. These facts seemed to support the view that thermal shape fluctuations are essentially shear-free (see discussion).

In principle one should be able to infer the bending modulus k_c from the distortion of the equilibrium shape due to adhesive forces (Seifert and Lipowsky, 1992). In that context it would be interesting to find out whether the apparent linear relationship between the bending modulus and the thickness of the annular ring (see Fig. 10) can be confirmed theoretically. As there is not very much known about adhesive contacts between cell surfaces and solid substrates as in this case, one should be able to use the bending modulus measured by us and estimate adhesion energies from that.

On the assumption that the mode with $m = 0$ should be unobservably small the measured mode $\langle \delta n^2_{m=0} \rangle$ must be compared with the theoretical amplitude $\langle \delta N^2_{m=4} \rangle$ because of aliasing (see Materials and Methods). All measured amplitudes $\langle \delta n^2_{m=0} \rangle$ were in reasonable agreement with theoretically predicted amplitudes $\langle \delta N^2_{m=4} \rangle$.

All three modes could be explained by the proposed model, in which we only used two to calculate the elastic constants k_c and μ. The third mode independently fitted very well with the theoretically predicted one, which strongly indicates that our proposed model explains the flicker motion of RBCs adhered to a coverslip.

Influence of diamid on membrane elasticity

Because the observed cells were adhered to the bottom coverslip it was possible to change the chemical composition of the buffer using a flow chamber as previously described (Zeman et al., 1990). The experimental setup allowed us to monitor both bending elasticity k_c and shear modulus μ while changing buffer conditions.

To demonstrate the application of our method we performed a single experiment with diamid (Sigma Chemical Co., St. Louis, MO), which cross-links proteins by forming sulfur bridges. A diamid concentration of 0.1 mg/ml is known to increase the shear elasticity μ by a factor of three (shear flow method, Fischer et al., 1978), whereas a concentration of 1 mg/ml increases μ by a factor of 8 (electrical field deformation; Engelhardt and Sackmann, 1988).

Fig. 11 shows the time evolution of both bending elasticity k_c and shear elasticity after treatment with diamid. The first arrow in Fig. 11 indicates when buffer with diamid concentration of 0.1 mg/ml was injected into the flow chamber. After injection all cells immediately showed slight echinocytosis. 20 min later most of the cells relaxed to discocytes again. The bending modulus k_c of the measured RBC then increased continuously with time. The shape of the time evolution suggests that k_c saturates after ~60 min at a value that was ~30% larger than for the untreated cell.

Fig. 11 (*second arrow*) shows the point at which buffer with diamid concentration of 1 mg/ml was injected, which increased the bending stiffness k_c. At 120 min the bending modulus dropped again and shortly after that the measured RBC became an echinocyte and was therefore no longer accessible for further measurements.

Surprisingly the time evolution of the shear modulus μ did not show the expected significant increase, which additionally supported our view that the shear resistance of the cytoskeleton does not influence the flicker motions (see Discussion). This result also agreed with previous flicker experiments in our lab (Zeman et al., 1990).

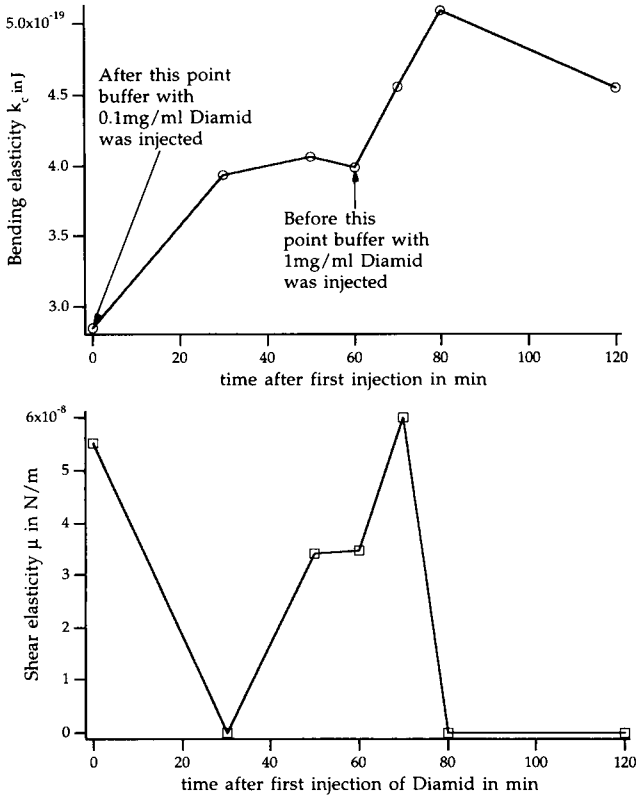

FIGURE 11 Time course of both bending k_c and shear elasticity μ of a RBC after treatment with diamid. After the first injection of 0.1 mg/ml diamid most RBCs showed slight echinocytosis which relaxed after 20 min. The bending stiffness k_c then increased continuously by ~30%. The shape of the time course suggests a saturation effect of the bending stiffness after 60 min. After 60 min 1 mg/ml diamid was injected, which increased k_c again. After 120 min the measured RBC became an echinocyte. Interestingly, the shear elasticity did not increase as expected from micromechanical measurements, indicating that flicker motions are shear-free.

DISCUSSION

The erythrocyte flicker phenomenon is understood to be the Brownian shape fluctuation of the RBC membrane (Brochard and Lennon, 1975; Zeman et al., 1990; Peterson et al., 1992). Its mean square amplitude is a non-invasive measure of the elastic properties of the membrane, and hence of considerable interest. Quantitative measurements of flicker have been used to infer the bending modulus k_c of the membrane.

One outstanding question in the interpretation of flicker measurements is the role of the shear modulus μ of the cytoskeleton. Early analyses modeled the membrane as flat and ignored μ, because out-of-plane motions of a flat membrane produce shear strain only in second order. This argument is plausible for very short wavelength shape fluctuations, a regime that has been studied by reflection interference microscopy, (Zilker et al., 1992b) but not for wavelengths comparable to the cell size. On this length scale the membrane is curved, and out-of-surface displacements produce shear strain in first order. Thus μ ought to influence the large scale flicker amplitudes after all. In fact, if μ were as large as the value inferred from micromechanical experiments (Hochmuth, 1987), flicker amplitudes should be much smaller. This issue has never been resolved.

It is likely that the shear stress-strain relationship is very nonlinear. In micromechanical experiments the maximum shear extension ratio typically ranges from 1.5 to 2.5 (Waugh and Evans, 1979). In the flicker experiment, where normal displacements of the membrane result in shear deformations, the shear extension ratio is $\delta n/R$, where R is the radius of the cell. Using δn = 90 nm as an estimate for the maximal normal displacement (three times the standard deviation) and R = 3 μm, the maximal shear extension ratio is 0.03 or 3%, which is almost two orders of magnitudes smaller than the value for micropipette experiments. It would be even more legitimate to talk about harmonic deformations in our case, because the deformations are so small. Still it was puzzling that μ in flicker seemed to be zero.

We have found the m = 1 mode to be the dominant mode, contrary to the conclusions of our first paper (Peterson et al., 1992). In our previous analysis we ascribed the large amplitude near the rim to the l = 2,m = 2 shape mode, which is an approximate Goldstone mode of the μ = 0 vesicle. (i.e., a mode which is soft because of a symmetry) (Peterson, 1992). This m = 2 mode is very sensitive to μ. It was argued that the translation mode, which is l = 1,m = 1, and really is a Goldstone mode, should be omitted from the analysis, because the cells were attached to a rigid substratum.

As noted above, we have now decomposed the observed fluctuations at the rim of the cell according to the azimuthal number m, and the largest mode is not m = 2 as it should be according to the earlier analysis, but m = 1. The reason is perhaps obvious in retrospect. The translation mode is not eliminated by the attachment to the substratum. Rather, a constraint is introduced on one side of the cell, and reflection symmetry is broken. The translation mode survives as a hindered translation, a large amplitude m = 1 mode, still an approximate Goldstone mode. Curiously, the thickness fluctuation profile obtained in this way is almost indistinguishable from the μ = 0 profile with translation omitted. Thus the mode decomposition was crucial for a real, detailed understanding of flicker, and only with this decomposition could one see clearly the effect of non-zero μ.

This detailed analysis enables us to assign a value to k_c that is free of the theoretical uncertainties of previous analyses, because we can now be confident we have described the shape fluctuations exactly. Both measurements at short wavelengths with RICM (Zilker et al., 1992b) and the original analysis of Brochard and Lennon (1975) found a value of k_c in erythrocytes that was less than k_c measured for pure lipid bilayers, a puzzle that now seems to be solved: k_c for the erythrocyte in the long wavelength regime is not anomalous after all.

From our experimental flicker amplitude of about 900 nm^2 at the rim of the cell $\langle \delta n^2 \rangle$ we can estimate an upper

cutoff for the bending elasticity k_c from a plane wave approximation. The mean square height fluctuations of a membrane with total area A is given by Helfrich and Servuss (1984).

$$\langle \delta h^2 \rangle = \frac{k_B T}{2\pi k_c} q_{min}^{-2} = \frac{A k_B T}{8\pi^3 k_c} \quad (3)$$

with the lower cutoff wavevector $q_{min} = 2\pi/A^{1/2}$. Using the total area of a red cell membrane of $A = 135\ \mu m^2$ yields a bending modulus $k_c = 2.5 \times 10^{-18}$ J.

The real bending elasticity is reduced for the following two reasons. 1) The constraints of fixed area and fixed volume hinder long wavelength modes (see Appendix). Therefore, q_{min} is getting larger, and for the same mean square height fluctuation a smaller bending modulus results from Eq. 3. 2) A non-zero shear elasticity reduces the flicker amplitude independently. The resulting bending elasticity is smaller.

Nevertheless, the resulting k_c of 2–7 $\times 10^{-19}$ J is large compared with red cell membrane bending moduli reported by other authors. Evans (1983) estimated an upper limit for the bending modulus of $k_c = 1.8 \times 10^{-19}$ J from the critical micropipette aspiration pressure at which erythrocytes buckled. A much smaller value of the bending modulus of erythrocytes of $k_c = 2.3 \times 10^{-20}$ J was reported recently by Zilker et al. (1992b). These researchers measured the short wavelength excitations ($1\ \mu m^{-1} < q < 4\ \mu m^{-1}$) by RICM and analyzed them according to Brochard and Lennon (1975) as thermally excited plane waves. Their value is almost 20 times smaller than our average value. This would lead to a 20 times larger mean square amplitude, which should then be easily observable. One reason to explain this extremely small value could be that for small wavelengths ATP-consuming cell metabolic processes such as phosphorylation and dephosphorylation of the cytoskeleton play a role. This aspect has been discussed recently by us (Zilker et al., 1992a). On the other hand it seems to be reasonable that the bending modulus should decrease with decreasing wavelength because of the finite bond length of the cytoskeleton (~80 nm). Below this bond length the bending modulus should be that of the pure lipid bilayer, whereas above this length the red cell membrane has to be considered as composite material of lipid bilayer plus cytoskeleton.

The contribution of the spectrin network to the bending modulus is still unclear. In general the bending elastic modulus for a uniform material can be calculated by $k_c = Kh^2$, where K is the area compressibility modulus, h is its thickness. For layered material this equation has to be modified depending on whether the different layers can slide against each other. Assuming that all the layers have the same K the previous equation has to be modified by a prefactor smaller than one (see, e.g., Evans and Skalak, 1980). A strong upper limit for the contribution to k_c would therefore be $(6 \times 10^{-6}\text{N/m},) \times (30\text{ nm})^2 = 5.4 \times 10^{-21}$ J, where we used Waugh and Evans' (1979) shear modulus μ for K ($K = C\mu$ with C in the order of 1) and 30 nm as an estimate for the thickness of the spectrin layer. This shows that the spectrin network should not contribute to the bending elasticity at all. On the other hand our diamid experiment clearly showed that cross-linking the proteins of an erythrocyte increased bending elasticity. Perhaps the elasticity of intramembrane proteins influences the bending modulus. Because 45% of the red cell membrane consists of proteins this seems plausible.

One question now remains unanswered. Why is the bending stiffness k_c of red cell membranes two to seven times larger than the k_c of DMPC? We find the answer in the composition of an erythrocyte membrane, which consists of 40–50% w/w proteins, 35–45% w/w lipid, and 7–15% w/w carbohydrates. The lipid fraction itself consists of 50 mol % phospholipids and 50 mol % cholesterol (Wissenschaftliche Tabellen Geigy, Blut).

A mixture of 1:1 DMPC:cholesterol is known to exhibit an area compressibility modulus K of 7×10^{-1}N/m, which is about five times larger than $K = 1.45 \times 10^{-1}$N/m, of pure DMPC (Needham, 1988). This means that using $k_c = Kh^2$, assuming that h does not change a bending modulus for erythrocytes five times that of DMPC could be explained by cholesterol. From the above argument one would expect a bending modulus for erythrocytes of 3×10^{-19} J from its area compressibility modulus of $K = 4.5 \times 10^{-1}$N/m, (Evans et al., 1976; Evans and Waugh, 1977). A bending modulus of 2–7 $\times 10^{-19}$ J seems therefore much more favorable than the 20 times smaller value of 2.3×10^{-20} J (Zilker et al., 1992b) for short wavelength excitations.

From the comparison of theory and experiment it seems that there is almost no shear involved. Since the shear moduli we obtain are so small that they can be addressed to uncertainties of the measured flicker amplitudes it seems more reasonable to assume that flicker is essentially shear-free.

To address the question about a vanishing shear modulus we first want to focus on what is known about the conformation of the cytoskeleton. The current view is that the cytoskeleton is a 2-dimensional triangular lattice formed by flexible spectrin tetramers (a tetramer consists of two spectrin dimers jointed by ankyrin), which are linked by actin oligomers (made of ~13 monomers) with an average side length of the triangles of ~70–80 nm (Liu et al., 1987). Since this side length is much smaller than the contour length of the spectrin tetramer of about 200 nm, it is believed that the spectrins essentially act as entropy springs.

The cytoskeleton couples to the lipid bilayer via intramembrane proteins. One binding site is the intramembrane protein band III, which couples to ankyrin. There is further evidence that the actin oligomers can couple to the membrane proteins glycophorin A–C mediated by band 4.1 (Steck, 1989; Bennett, 1990).

It is not clear, however, how strong these bonds are and how the bending constants of ankyrin to band III and band 4.1 glycophorin C influences the elastic properties. There is, e.g., an 80% mobile fraction of band III in the membrane,

which indicates that there could be a dynamic rearrangement of the spectrin bonds. This idea would be supported by measurement of the elastic modulus at short wavelengths, which resulted in a bending modulus of 2×10^{-20} J (Zilker et al., 1992b). If short wavelength excitations have to do with phosphorylation and dephosphorylation reactions changing the binding energies in the cytoskeleton, then both values could be explained. The low bending rigidity of 2×10^{-20} J would then be an active (ATP-driven) motion of the cell membrane, and our value represents the global bending rigidity of the membrane.

Several theoretical attempts have been made to explain the elastic properties of the cytoskeleton. Stokke et al. (1986a,b) suggested that the membrane skeleton behaves like an ionic gel in order to explain its anomalous behavior of the shear elasticity with respect to temperature (Waugh and Evans, 1979). A different theoretical model was proposed by Kozlov and Markin (1987) and Markin and Kozlov (1988), which took into account that spectrin bonds can rearrange. Both models have been discussed and compared recently by Fischer (1992) with respect to their implications on the shear and area compressibility modulus of the cytoskeleton.

Recent Monte Carlo simulations of triangular lattices of entropy springs indicate that for a perfect lattice of entropy springs coupled to a membrane the erythrocyte shear modulus should be 10×10^{-6}N/m, (Boal, 1994), significantly bigger than the micropipet aspiration value of $6.6 \times 10^{-6} N/m$,. The shear modulus was determined by analyzing the lateral mean square fluctuations of the network, exactly the way we would sense shear elasticity in our measurements, and therefore is in strong disagreement with our findings.

Other simulations have modeled the cytoskeleton by surface-tethered self-avoiding chains in a good solvent (Everaers, R., I. S. Graham, E. Sackmann, and M. J. Zuckermann (1993) Elasticity of two and three dimensional polymer gels in a good solvent under external pressure, and Entropic elasticity and end-to-end distance distributions of free and surface tethered polymer chains, unpublished articles). These chains are stretched when they are relaxed and show nonlinear behavior. This nonlinear force law could indeed explain that the shear modulus is much smaller for small deformations.

It is interesting to note that if the cytoskeleton were easily compressed, i.e., had essentially zero compressibility modulus, then it could completely relax shear strain associated with normal displacement. This means that even though the cytoskeleton might still have an appreciable shear modulus, the shear modulus would not influence the flicker modes. We found this result in a computation of modes with compressible cytoskeleton, but it is easy to understand why it is true. In two dimensions the traceless part of the strain tensor has only two independent components. Without the constraint of local incompressibility we can choose the two tangential components of displacement to annul the traceless shear strain produced by the normal displacement (see Appendix).

Because the cytoskeleton, in the absence of interaction with the lipid bilayer, would have a compressibility modulus comparable to its shear modulus, this mechanism could only work if the (isotropic) fluid bilayer compensated the isotropic stress of the cytoskeleton, at least in some small region close to equilibrium.

It is not clear yet which model would be favorable to describe the mechanical properties of the red cell membrane, but to develop a satisfactory model one should also consider the following point. Our flicker measurement of red cells did not show any influence of lateral tension (tension would significantly change the ratio between the first two modes). For this there are two possible explanations.

1) The cytoskeleton is relaxed and exerts no tension on the lipid bilayer. This would be in agreement with experiments on isolated erythrocyte spectrin networks (Svoboda et al., 1992), which under physiological salt concentrations showed almost the same surface area as the intact membrane, indicating low lateral tension.

2) The other explanation would be that although the cytoskeleton is under entropic tension, the lipid bilayer somehow compensates for this lateral tension. This compensation could arise from local bending of the bilayer between spectrin bonds. In fact such preundulations have been observed by electron microscopy of erythrocyte membranes with a wavelength of ~100 nm, which also indicates that the bilayer surface area exceeds the area of the cytoskeleton (Zeman et al., 1990; Zilker et al., 1992a). Another compensation mechanism could arise from spontaneous curvature induced by transmembrane lipid asymmetry created by flipases (Devaux, 1993). It seems obvious that this coupling then also plays a crucial role for the elastic response of the red cell membrane to stress and the red cell membrane would have to be modeled as a composite material.

APPENDIX

Constrained modes

The elastic properties of the red cell membrane was modeled as a membrane with a bending modulus k_c, a shear modulus μ, and an infinite lateral compressibility modulus, which kept the local area density of the mem-

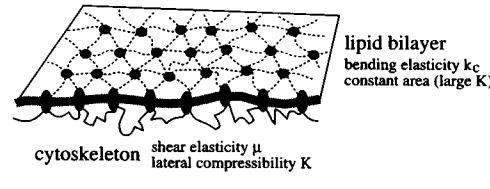

FIGURE 12 Schematic picture of an erythrocyte membrane. The cytoskeleton is coupled to the fluid-lipid bilayer through intramembrane proteins. The lipid bilayer is responsible for the bending elasticity k_c of the compound membrane, whereas the cytoskeleton contributes with its shear elasticity μ and its lateral compressibility modulus K. The total area is fixed because of the lateral incompressibility of the lipid bilayer.

brane fixed. Fig. 12 shows a schematic picture of a red cell membrane. The fluid lipid bilayer is responsible for the bending modulus of the composite membrane, whereas the cytoskeleton contributes with its shear resistance. The large lateral compressibility modulus of the bilayer holds the total area of the red cell membrane fixed. We showed in earlier calculations that as long as the lateral compressibility modulus K of the cytoskeleton is on the same order of magnitude or larger than the shear modulus the long wavelength eigenmodes are purely dominated by bending and shear deformations (M. Peterson, unpublished results). This can be easily understood given that large wavelength modes that would involve lateral compression of the cytoskeleton are suppressed by the global area constraint, whereas for pure shear the local area density stays constant. Inasmuch as there are strong indications that the lateral compressibility modulus of the cytoskeleton is about twice as large as its shear modulus (Boal, 1994; Discher et al., 1995), it is legitimate to assume an infinite lateral compressibility K, which simplified the theoretical calculations significantly.

A method for computing shape eigenmodes of erythrocytes has been described already (Peterson et al., 1992; Peterson, 1992). We review it only briefly here, because what is new in this analysis is just one additional energy term describing the attachment to the substratum.

At equilibrium, the elastic energy of the erythrocyte is a minimum, so its first variation, subject to constraints, vanishes.

$$\delta E = 0 \tag{4}$$

The second variation $\delta^2 E$ is a quadratic form in the (linear) space of motions that obey the constraints to first order, but this is a linear subspace of the space of all first order motions, because the constraints are themselves linear in first order. For example, the constant volume constraint implies that the normal displacement of the membrane must be orthogonal to the constant function, i.e.,

$$\int N(s,\Psi)\, dA = 0 \tag{5}$$

where n is the normal displacement. Similarly the constant area constraint is

$$\int N(s,\Psi) H dA = 0 \tag{6}$$

where H is the mean curvature. Following is the bilayer coupling hypothesis, which is the constraint that $\langle H \rangle$, the average value of H, be constant, and which is called equivalent to the conservation of area in each monolayer separately.

$$\int N(s,\Psi)\, K dA = 0 \tag{7}$$

where K is the Gauss curvature. One deals with these constraints by pulling the quadratic form back to the corresponding subspace and diagonalizing it there. In this way we predicted, correctly, that certain $m = 0$ displacements would not occur. The effect is approximately to remove $Y_{00}(s, \psi)$, $Y_{20}(s, \psi)$, and, in case the bilayer coupling hypothesis is correct, $Y_{40}(s, \psi)$ from the allowed modes for n. Because the only modes that are not zero at the center of the cell are the $m = 0$ modes, and because the constraints forbid the lowest ones, flicker amplitudes at the center of the cell should be relatively small, and this is indeed the case.

To describe the attachment to the substratum we now add a harmonic potential in normal displacement n at those points on the erythrocyte surface where the attachment occurs. This makes normal displacement in the attachment region energetically expensive, but not strictly forbidden. This term breaks reflection symmetry in the equatorial plane of the cell. Because the attachment region is a ring, however, the modes still have azimuthal symmetry. The computation now goes exactly as before. The energy eigenmodes are found by diagonalizing the second variation, considered as a quadratic form in admissible displacements of the membrane, a space that now includes both even and odd reflection symmetry.

Because we do not know the strength of the attachment, we have done this computation for a range of harmonic potential strengths, from 10^7 to 10^{11} in units where $k_c = 1$ and the effective radius of the cell $R = 1$. We look for a limiting behavior as the strength of the confining harmonic potential increases. This limiting behavior sets in at about 10^8. We also vary the way we truncate the space of admissible modes, and require that the result be insensitive to this truncation. This typically requires that we keep many more modes than are necessary to describe a free-swimming cell, because the true modes are essentially zero over the attachment region. Keeping too few modes leads to an artificially high energy, because in such a space there is necessarily too much displacement in the attachment region. Limiting behavior typically sets in when the dimension of the admissible space of normal displacements is 40–50, in case the discretized cell form is described by 64 regularly spaced points between the azimuthal poles.

The modes are found under the assumption that the membrane, including the cytoskeleton, is locally incompressible. This implies that there is shear strain associated with normal displacement. We include tangential incompressible flows in the space of admissible motions in case the shear modulus is not zero: this doubles the dimension of the space we are working in, and gives the model cell additional degrees of freedom to minimize shear energy. It turns out that the cell cannot entirely relax shear strain within the constraint of local incompressibility. This is why the shear modulus influences the flicker modes.

This work was funded by the Deutsche Forschungsgemeinschaft (Sa 246/20) and the Fonds der Chemischen Industrie. H. S. is grateful for research fellowships from the National Institutes of Health and from the Deutsche Forschungsgemeinschaft. Helpful discussions with D. Boal, E. Evans, M. Kozlov, R. Podgornik, A. Parsegian, and U. Seifert are gratefully acknowledged. Special thanks to D. Lerche for donating blood.

REFERENCES

Bennett, V. 1990. Spectrin-based membrane skeleton: a multipotential adaptor between plasma membrane and cytoplasma. *Physiol. Rev.* 70: 1029.

Boal, D. H. 1994. Computer simulation of a model network for the erythrocyte cytoskeleton. *Biophys. J.* 67:521–529.

Brochard, F., and J. F. Lennon. 1975. Frequency spectrum of the flicker phenomenon in erythrocytes. *J. Physique.* 11:1035.

Devaux, P. F. 1993. *Curr. Opin. Struct. Biol.* 3:489–494.

Discher, D. E., N. Mohandas, and E. Evans. 1995. Molecular maps of red cell deformation: hidden elasticity and in situ connectivity. *Science.* In press.

Duwe, H. P., J. Käs, and E. Sackmann. 1990. Bending elastic moduli of lipid bilayers : modulation by solutes, J. *Phys. France* 51:945–962.

Engelhardt, H., and E. Sackmann. 1988. On the measurement of shear elastic moduli and viscosities of the erythrocyte plasma membranes by transient deformation in high frequency electric fields. *Biophys. J.* 54: 495–508.

Evans, E. A. 1983. Bending elastic modulus of red blood cell membrane derived from buckling instability in micropipet aspiration tests. *Biophys. J.* 43:27–30.

Evans, E. A., and R. Skalak. 1980. Mechanics and Thermodynamics of Biomembranes. CRC Press, Boca Raton, FL.

Evans, E. A., and R. Waugh. 1977. Osmotic correction to elastic area compressibility measurements on red cell membrane. *Biophys. J.* 20: 307.

Evans, E. A., R. Waugh, and L. Melnik. 1976. Elastic area compressibility modulus of red blood cell membrane. *Biophys. J.* 16:585–595.

Faucon J. F., Mitov M. D., Méléard P., Bivas I., and Bothorel P. 1989. Bending elasticity and thermal fluctuations of lipid membranes. Theoretical and experimental requirements. *J. Phys. France.* 50: 2389–2414.

Fischer, T. M. 1992. Is the surface area of red cell membrane skeleton locally conserved? *Biophys. J.* 61:292–305.

Fischer, T. M., C. W. M. Haest, M. Stör, D. Kamp, and B. Deuticke. 1978. Selective alteration of erythrocyte deformability by SH-reagents. Evidence for an involvement of spectrin in membrane shear elasticity. *Biochim. Biophys. Acta.* 510:270–282.

Helfrich, W., and R.-M. Servuss. 1984. Undulations, Steric Interaction and Cohesion of Fluid Membranes, Il Nuovo Cimento 3D:137–151.

Hochmuth, R. M. 1987. Properties of red blood cells. *In* Handbook of Bioengineering. R. Skalak and S. Chien, editors. McGraw-Hill, New York.

Hochmuth, R. M., N. Mohandas, and P. L. Blackshear Jr. 1973. Measurement of the elastic modulus for red cell membrane using a fluid mechanical technique. *Biophys. J.* 13:747–762.

Inoué, S. 1989. Imaging of unresolved objects, superresolution, and precision of distance measurement with video microscopy. *Methods Cell Biol.* 30:85–112.

Kozlov, M. M., and V. S. Markin. 1987. Model of red blood cell membrane skeleton: electrical and mechanical properties. *J. Theor. Biol.* 129: 439–452.

Linderkamp O., and H. J. Meiselman. 1982. Geometric, osmotic, and mechanical properties of density-separated human red cells. *Blood.* 59:1121–1127.

Liu, S., Derick, L. H., and J. Palek. 1987. Visualization of the hexagonal lattice in the erythrocyte membrane skeleton. *J. Cell Biol.* 104:527–536.

Needham, D., McIntosh, T. J., and E. A. Evans. 1988. Thermomechanical and transition properties of DMPC: cholesterol bilayers. *Biochemistry.* 27:4668–4673.

Markin, V. S., and M. M. Kozlov. 1988. Mechanical properties of the red cell membrane skeleton: analysis of axisymmetric deformations. *J. Theor. Biol.* 133:147–167.

Peterson, M. A. 1985. Geometrical methods for the elasticity theory of membranes. *J. Math. Phys.* 26:711.

Peterson, M. A. 1992. Linear response of human erythrocytes to mechanical stress. *Phys. Rev. A.* 45:4116.

Peterson, M. A., H. Strey, and E. Sackmann. 1992. Theoretical and phase contrast microscopic eigenmode analysis of erythrocyte flicker: amplitudes. *J. Phys. II France.* 2:1273–1285.

Press, W. H., B. P. Flannery, S. A. Teukolsky, and W. T. Vetterling. 1988. Numerical Recipes in C, Cambridge University Press, Cambridge, UK.

Rädler, J., and E. Sackmann. 1993. Imaging optical thicknesses and separation distances of phospholipid vesicles at solid surfaces. *J. Phys. II France.* 3:727–748.

Reichl, L. E. 1980. A Modern Course in Statistical Physics. Edward Arnold, Kent, UK.

Seifert, U., and R. Lipowsky. 1992. Adhesion of vesicles. *Phys. Rev. A* 42:4768–4771.

Steck, T. L. 1989. Red Cell Shape, Cell Shape: Determinants, Regulation, and Regulatory Role. Academic Press, New York.

Stokke, B. T., A. Mikkelsen, and A. Elgsaeter. 1986a. The human erythrocyte membrane skeleton may be an ionic gel. I. Membrane mechanochemical properties. *Eur. Biophys. J.* 13:203–218.

Stokke, B. T., A. Mikkelsen, and A. Elgsaeter. 1986b. The human erythrocyte membrane skeleton may be an ionic gel. III. Micropipette aspiration of unswollen erythrocytes. *J. Theor. Biol.* 123:205–211.

Svoboda, K., C. F. Schmidt, D. Branton, and S. M. Block. 1992. Conformation and elasticity of the isolated red blood cell membrane skeleton. *Biophys. J.* 63:784–793.

Waugh, R., and E. A. Evans. 1979. Thermoelasticity of red blood cell membrane. *Biophys. J.* 26:115–132.

Zeman, K., H. Engelhardt, and E. Sackmann. 1990. Bending undulations and elasticity of the erythrocyte membrane: effects of cell shape and membrane organization. *Eur. Biophys. J.* 18:203–219.

Zilker, A., H. Strey, and E. Sackmann. 1992a. Erythrocyte membranes: tethered shells with fluid-like deformation regime: the structure and conformation of amphiphilic membranes. *Springer Proc. Physics.* 66.

Zilker, A., M. Ziegler, and E. Sackmann. 1992b. Spectral analysis of erythrocyte flickering in the 0.3–4 μm-1 regime by microinterferometry combined with fast image processing. *Phys. Rev. A.* 46:7998–8001.